Available online at www.sciencedirect.com
ScienceDirect
Scripta Materialia 58 (2008) 311–314
Scripta MATERIALIA
www.elsevier.com/locate/scriptamat

Network-shaped fine-grained microstructure and high ductility of magnesium alloy fabricated by cyclic extrusion compression

Y.J. Chen,[a] Q.D. Wang,[a,*] H.J. Roven,[b] M.P. Liu,[b] M. Karlsen,[b] Y.D. Yu[b] and J. Hjelen[b]

[a] *State Key Laboratory of Metal Matrix Composites, Shanghai Jiaotong University, Shanghai 200030, China*
[b] *The Norwegian University of Science and Technology, Department of Materials Technology, 7491 Trondheim, Norway*

Received 28 June 2007; revised 26 August 2007; accepted 29 September 2007
Available online 5 November 2007

An extraordinary microstructure with mean grain size of 1.77 μm accompanying fine grains of 150 ± 50 nm was obtained for magnesium alloy AZ31 by cyclic extrusion compression (CEC). The ductility improved 2.2 times while yield strength decreased 50 MPa after CEC 7 passes compared with as-extruded alloy. A compound grain-refining mechanism was proposed to explain the microstructure evolution during CEC. Dislocation density, texture and grain-boundary structure were employed to clarify the relationship between microstructure and mechanical properties of AZ31 alloy after CEC.

Keywords: Magnesium alloys; Grain-refining; Electron backscatter diffraction (EBSD); Cyclic extrusion compression (CEC); Mechanical properties

Magnesium alloys are potential candidates for replacing steel and other high-specific-weight materials due to their low density and high-specific strength [1]. Nevertheless, the application of wrought magnesium alloys is limited by its low room temperature ductility [2]. New efforts on grain refinement are devoted to minimizing these disadvantages. Among them, severe plastic deformation (SPD), aimed at the fabrication of massive bulk nanostructured materials (NSM) or ultrafine-grained microstructure (UFG, grain size in the range 100–1000 nm) materials, has been successfully used to obtain fine-grained magnesium alloys [3–6]. CEC [5], as a kind of continuous SPD technique, is very suitable for refining grains of hard-deformation metals due to the materials imposed by three-dimensional compression stress during the CEC process. However, there are few reports on microstructure and mechanical properties of fine-grained magnesium alloys fabricated by CEC. Moreover, the grain-refining mechanism during CEC is still unknown up to now. The present work reveals the extraordinary microstructure and mechanical properties of Mg alloys after the CEC process and clarifies the grain-refining mechanism of magnesium alloys during CEC.

The Mg alloy AZ31 (Mg–3.1%Al–1.0%Zn–0.4%Mn, by wt.%) was used in the as-extruded condition. Both the extruded bar workpiece and the die were held for 10 min at 100 °C and coated with a lubricant of graphite powder before heating to 300 °C for about 2 h. The sample was put into the upper chamber to start the CEC processing cycle [5,7]. The CEC passes 1, 3 and 7 were applied, corresponding to equivalent strains 0.81, 4.1 and 10.5, respectively [5]. After processing, longitudinal sections were prepared for transmission electron microscopy (TEM) observation and electron backscatter diffraction (EBSD) analyses in the scanning electron microscope. The average confidence indexes (CI) after cleanup are 87%, 83%, 78% and 77% for as-extruded, and CECed AZ31 of 1, 3 and 7, respectively.

Figure 1 shows the grain-boundaries map of as-extruded and processed CEC alloy. The low-angle grain-boundaries (LAGBs, between 2° and 15°) and high-angle grain-boundaries (HAGBs) are marked by thin and thick black lines, respectively. There are numerous LAGBs in the as-extruded material, as shown in Figure 1a. Figure 1b shows that the LAGBs seem to evolve into HAGBs and finer grains are achieved. The fine grains gather together to form network-shaped structures. With the increase of accumulated strain, the fraction of grain-boundaries increases (see Fig. 1c). The network-shaped structure is subdivided and more network-shaped structures are formed. When the alloy

* Corresponding author. Tel.: +86 21 62933139; fax: +86 21 62932113; e-mail: wangqudong@sjtu.edu.cn

1359-6462/$ - see front matter © 2007 Acta Materialia Inc. Published by Elsevier Ltd. All rights reserved.
doi:10.1016/j.scriptamat.2007.09.058

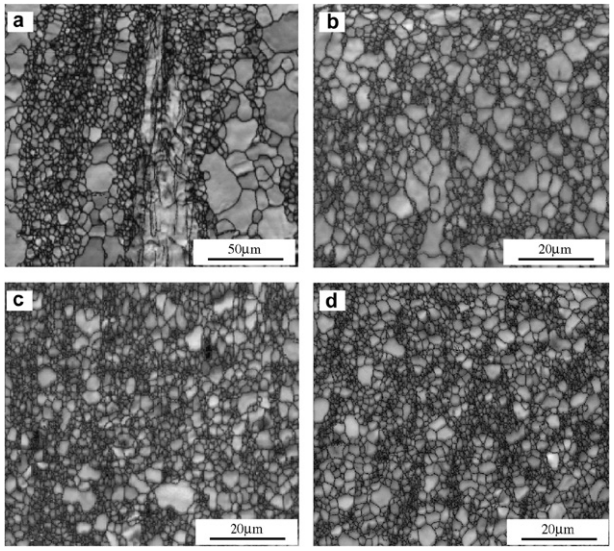

Figure 1. Grain boundaries map (SEM-EBSD) of as-extruded and alloys processed by CEC at 573 K: (a) as-extruded; (b) CEC 1 pass; (c) CEC 3 passes; (d) CEC 7 passes.

is deformed to 7 passes (Fig. 1d), the distribution of network-shaped structures is more homogeneous and the residual coarse grains are separated by the network-shaped structure.

Figure 2 shows typical distribution histograms of grain size for as-extruded alloys and alloys processed by CEC. Compared with the distribution of grain size of as-extruded AZ31 alloy (Fig. 2a), one can clearly find that the grain refinement takes place mainly during CEC 1 pass and the grain size decreases slowly with further increasing strain. The mean grain size of AZ31 alloy is about 2.17 μm after CEC 1 pass (seen in Fig. 2b). After CEC 3 passes the distribution of grain size tends to be more homogeneous and the mean grain size is nearly 1.89 μm (seen in Fig. 2c). With further deformation, the mean grain size reaches 1.77 μm after CEC 7 passes (seen in Fig. 2d).

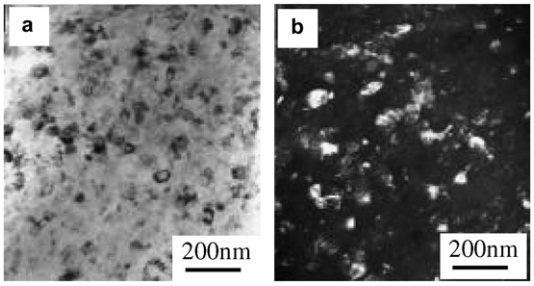

Figure 3. TEM micrographs of AZ31 alloy after CEC 7 passes and 573 K: (a) bright field; (b) corresponding dark field.

In order to confirm the grain size of fine grains, which is difficult to distinguish by EBSD due to the applied scan step, TEM was performed to obtain detailed information. The grain size of fine grains of AZ31 alloy after CEC 7 passes is in the range 150 ± 50 nm, as can be seen in Figure 3a and b. It is interesting to note that there are many {10–12} twins in the microstructure of CEC 1 and 3 passes (seen in Fig. 4) while it is difficult to find any twins in the microstructure of CEC 7 passes.

Table 1 summarizes the average misorientation, fraction of LAGBs, texture, texture intensity and the calculated maximum Schmid factor for as-extruded and CEC samples. The average misorientation clearly increases from 34.6 of as-extruded to 50.9 of CEC 1 pass. Then it tends to increase as CEC pass increases. Both the fraction of LAGBs and texture intensity tend to decrease with the increase of CEC pass. One can clearly see that the {0001} crystal plane is parallel to viewing plane at CEC 1 pass. The angle between {0001} crystal plane and viewing plane increases from 0° of CEC 1 passe to 73° of CEC 3 passes. After CEC 7 passes, it is 90°, which means the {0001} crystal plane is normal to extrusion direction. The change of texture shows that the big angle rotation for grains happens during CEC deformation. The calculated maximum Schmid factor shows that it is difficult to deform for as-extruded and CEC 1 pass, but easy for CEC 3 passes and 7 passes.

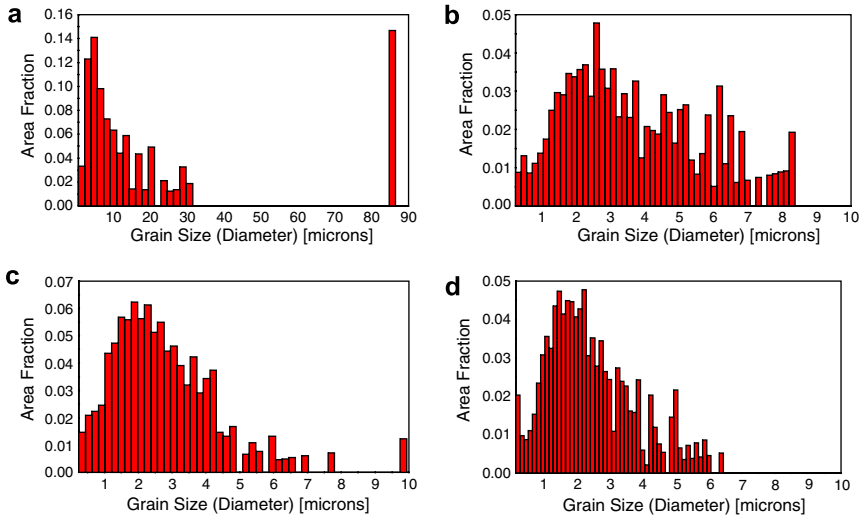

Figure 2. Grain-size distribution of as-extruded alloys and alloys processed by CEC at 573 K: (a) as-extruded; (b) CEC 1 pass; (c) CEC 3 passes; (d) CEC 7 passes.

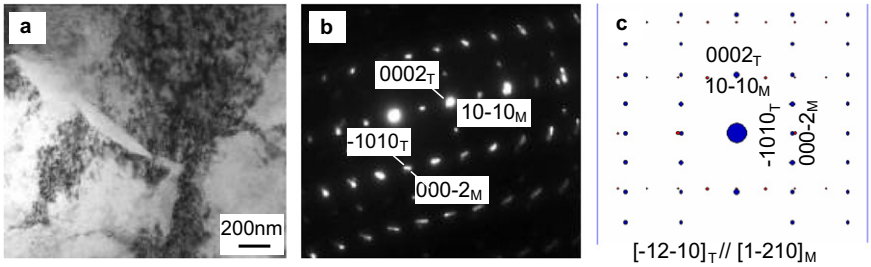

Figure 4. {10–12} twin in AZ31 alloy processed by CEC 3 passes and 573 K: (a) micrograph; (b) diffraction patterns of matrix and twin; (c) computer simulation of diffraction pattern of matrix and twin.

Table 1. Average misorientation, fraction of LAGBs, texture and maximum Schmid factor for CEC sample

CEC pass number	Average misorientation	Fraction of LAGBs (%)	Texture	Texture intensity	Maximum Schmid factor
0	34.6	28.7	$\{01-11\}\langle 2-1-10\rangle$	13.613	0
1	50.9	9.4	$\{0001\}\langle 1-100\rangle$	5.907	0
3	48.5	10.6	$\{-12-11\}\langle 3-1-23\rangle$	4.492	0.49
7	54.8	7	$\{14-50\}\langle 3-2-13\rangle$	4.488	0.49

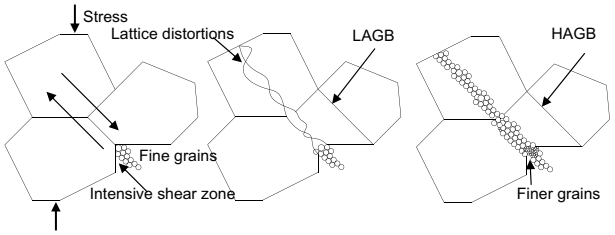

Figure 5. Schematic showing the grain refinement of magnesium alloys during CEC process (increasing strain accumulation going to the right).

Based on EBSD and TEM observation as well as the data summarized in Table 1, a compound grain-refining mechanism for magnesium alloys during CEC process can be proposed, and this is schematically shown in Figure 5. Firstly, the basal plane {0001} is mainly parallel to extrusion direction after extrusion while it is perpendicular to the compressed direction after compression [8,9]. Therefore, the basal planes have the tendency to periodically change during CEC processing. This explains the weakness of texture intensity with increasing CEC pass number (seen in Table 1). As usual, the large rotation cannot be achieved by slip alone. Thus the {10–12} twin is activated to correspond to the large angular rotations of the basal plane (seen in Fig. 4) [1,10–12]. Intensive shear stresses are imposed on grain-boundaries and grains due to the rotation tendency of basal plans. In this case, fine grains are easy to deform while with coarse grains this is more difficult. Thus lattice distortions occur at the boundaries between coarse grains and fine grains where stress concentrations are high enough, e.g. both along grain-boundaries and inside grains. Subgrains might form in the distorted regions where slip in non-basal systems may operate, thus giving rise to rotated regions and accommodating the external deformation. As strain increases further, which in turn develop into new grains. Such a mechanism could be viewed as a kind of rotational dynamic recrystallization (RDRX) [1,10]. The microstructure feature of fine grains gathering together to form network-shaped structures is in accordance with RDRX (seen in Fig. 1). Thirdly, LAGBs evolving into HAGBs as a kind of continuous dynamic recrystallization (CDRX) is suggested from TEM examinations in previous work [5]. Finally, during the time interval between passes, the CEC material experiences a thermal anneal at ~573 K. Thus static recovery and recrystallization are phenomena that are believed to occur. It can be expected that the grain structure cannot be substantially more refined due to both the grain-coarsening driven by the exposure to high temperature during extrusion/compression and in the time interval between passes and the decreasing grain-refining rate with the reducing coarse grains.

The measured 0.2% proof stress and elongation as a function of $d^{-1/2}$ is shown in Figure 6. The elongation increases from 16% of as-extruded to 17% of CEC 1 pass, then it increases sharply to 34% of CEC 3 pass; it is 2.2 times greater than as-extruded after CEC 7 passes. Yield strength increases from 189 MPa of as-extruded to 210 MPa of CEC 1 pass. Then it clearly decreases to 150 MPa of CEC 3 passes and decreases to 140 MPa after CEC 7 passes.

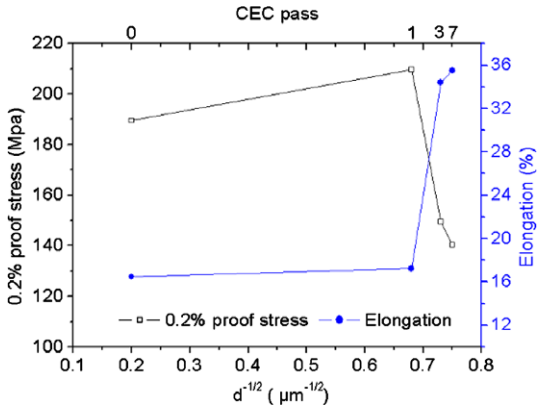

Figure 6. Measured 0.2% proof stress and elongation as a function of $d^{-1/2}$.

Strength and ductility of the fine-grained Mg alloy fabricated by CEC process were first clarified. The strength clearly presents an inverse Hall–Petch relationship after CEC process. This means that the strength of fine-grained Mg alloy after CEC is affected not only by grain size but also by dislocation density, texture and grain-boundary structure. The reason may be as follows: firstly, dislocation density in grains is very low after CEC process because repetitive extrusion and compression leads to the annihilation of dislocations with contrary sign (seen in Fig. 3), which means that the effect of dislocation strengthening in AZ31 alloy after CEC is not obvious. Secondly, the maximum Schmid factor of 0 at as-extruded alloy and CEC 1 pass shows that most grains in alloys are unfavorable to operate slip, which corresponds to high strength and low ductility (shown in Table 1 and Fig. 6). When the maximum Schmid factor increases sharply to 0.49 at CEC 3 and 7 passes, the critical resolved shear stress (CRSS) clearly decreases. Therefore yield strength should decrease and elongation increase. Lastly, the feature of fine grains, HAGBs and high average misorientation associated with AZ31 alloys after CEC may contribute to the grain-boundary sliding (GBS). Hauser et al. reported that GBS can operate at room temperature in UFG materials [13]. Recent research showed that GBS is easier to operate in finer grains, higher-angle grain-boundaries and higher average misorientation of Mg alloys [14,15]. GBS should decrease the stress concentration around grain-boundaries, therefore the strength decreases from CEC 1 pass to 7 passes. GBS and fine grains with high Schmid factor should improve the deformation compatibility of grain-boundaries and grains, respectively, which contribute to high ductility.

The present work firstly clarified the network-shaped fine-grained microstructure and extraordinary mechanical properties of AZ31 Mg alloy after CEC and provided evidence for the proposed compound grain-refining mechanism during CEC.

The present study was supported by the National Nature Science Foundation of the People's Republic of China under Grant No: 50674067.

[1] J.A. del Valle, M.T. Perez-Prado, O.A. Ruano, Mater. Sci. Eng. A 355 (2003) 68.
[2] M.D. Nave, M.R. Barnett, Scripta Mater. 51 (2004) 881.
[3] H.K. Lin, J.C. Huang, T.G. Langdon, Mater. Sci. Eng. A 402 (2005) 250.
[4] M. Mabuchi, K. Ameyama, H. Iwasaki, Acta Mater. 47 (1999) 2047.
[5] Y.J. Chen, Q.D. Wang, L.J. Zhang, J.B. Lin, C.Q. Zhai, J. Mater. Sci. 42 (2007) 7601.
[6] J. Xing, X.Y. Yang, H. Miura, et al., Mater. Sci. Forum 488–489 (2005) 597.
[7] J.W. Yeh, S.Y. Yuan, C.H. Peng, Mater. Sci. Eng. A 252 (1998) 212.
[8] T. Mukai, H. Watanabe, K. Ishikawa, K. Higashi, Mater. Sci. Forum 419–422 (2003) 171.
[9] H.L. Ding, L.F. Liu, S. Kamado, W.J. Ding, Y. Kojima, Mater. Sci. Eng. A (2006), doi:10.1016/j.msea.2006.10.091.
[10] S.E. Ion, F.J. Humphreys, S.H. White, Acta Metall. 30 (1982) 1909.
[11] L. Jiang, J.J. Jonas, A.A. Luo, A.K. Sachdev, S. Godet, Mater. Sci. Eng. A (2006), doi:10.1016/j.msea.2006.09.069.
[12] S.-B. Yi, C.H.J. Davies, H.-G. Brokmeier, R.E. Bolmaro, K.U. Kainer, J. Homeyer, Acta Mater. 54 (2006) 549.
[13] F.E. Hauser, P.R. Landon, J.E. Dorn, Trans. ASM 48 (1956) 986.
[14] L. Jin, Study on the microstructure and mechanical properties of magnesium alloy by equal channel angular extrusion, Shanghai, China, 2005, p. 115 (in Chinese).
[15] J. Koike, Mater. Sci. Forum 419–422 (2003) 189.